Article

Discovery Medicine 2025; 37(195): 706–714
https://doi.org/10.24976/Discov.Med.202537195.61

Effects of Botulinum Toxin A on Condylar Subchondral Bone Mass

Linqing Tian[1,2,†], Ye He[3,†], Wenli Zhang[4], Wenying Yang[5], Cong Jiang[6], Dongping He[5], Enyu Mao[2], Yingwei Luo[2,7,*], Xun Sheng[1,2,*]

[1]Department of Oral General, Kunming Medical University School and Hospital of Stomatology, 650106 Kunming, Yunnan, China
[2]Yunnan Key Laboratory of Stomatology, 650000 Kunming, Yunnan, China
[3]Physical Examination Management Center, The Second Affiliated Hospital of Kunming Medical University, 650033 Kunming, Yunnan, China
[4]Institute of Stomatology, Kunming Medical University Haiyuan College, 650106 Kunming, Yunnan, China
[5]Department of the Second Outpatient, Kunming Medical University School and Hospital of Stomatology, 650106 Kunming, Yunnan, China
[6]Department of Stomatology, The People's Hospital of Luxi, 652499 Honghe, Yunnan, China
[7]Department of Endodontics, Kunming Medical University School and Hospital of Stomatology, 650031 Kunming, Yunnan, China
*Correspondence: lyw@ydyy.cn (Yingwei Luo); kyshengxun@163.com (Xun Sheng)
[†]These authors contributed equally.
Published: 20 April 2025

Background: The management of temporomandibular disorders (TMD) remains challenging, with its underlying pathological mechanisms requiring further investigation. This study aimed to explore the effects of Botulinum Toxin A (Botox A) on the lateral pterygoid (LP) muscle and its impact on condylar subchondral bone mass.

Methods: Rats were randomly assigned to either an experimental group (injected with Botox A) or a control group (injected with an equal volume of 0.9% normal saline). All rats were sacrificed at 2-, 4-, 8-, or 12-weeks post-injection. The right condyles were harvested and analyzed using Micro-computed tomography (CT) scanning and hematoxylin-eosin staining to evaluate changes in the condylar subchondral bone. Osteoclast activity in the subchondral bone was assessed via tartrate-resistant acid phosphatase (TRAP) staining. The activities of osteoclasts and osteoblasts in subchondral bone were detected by western blotting.

Results: At 2-weeks post-Botox A injection, the trabecular number (Tb.N) was significantly lower ($p < 0.01$). At 2- and 4-weeks, bone volume fraction (BV/TV) and trabecular thickness (Tb.Th) were significantly lower ($p < 0.05$), while trabecular space (Tb.SP) and the ratio of bone surface area to bone volume (BS/BV) were significantly increased in the experimental group compared to control group ($p < 0.05$). At 8-weeks, BS/BV remained significantly elevated ($p < 0.05$), but no significant differences were observed in Tb.N, Tb.Th, BV/TV, or Tb.Sp at 8- and 12- weeks. Osteoclast numbers in the condylar subchondral bone were significantly higher in the Botox A group at 2-, 4-, and 8-weeks compared to the control group ($p < 0.05$). Additionally, protein expression levels of osteocalcin (OCN) and type I collagen (COL1A1) were markedly increased in the experimental group at 8- and 12-weeks ($p < 0.05$).

Conclusions: Botox A induces a significant reduction in condylar subchondral bone mass in rats during the early post-injection period, with subsequent time-dependent recovery.

Keywords: condyle; condylar subchondral bone; lateral pterygoid muscle; Micro-CT; temporomandibular joint

Introduction

The masticatory muscles play a pivotal role in the temporomandibular joint (TMJ) function, facilitating masticatory movements, and are anatomically composed of the masseter, temporalis, internal pterygoid, and lateral pterygoid (LP) muscles [1]. The TMJ connects the left and right sides of the maxillofacial region, forming an integrated masticatory system along with the masticatory muscles, teeth, vessels, and nerves [2]. Under normal physiological conditions, the TMJs on both sides exhibit structural and functional symmetry, ensuring balanced loading across the joint [3]. Temporomandibular disorder (TMD) encompasses degenerative musculoskeletal conditions arising from oral parafunctional activities, joint laxity, and masticatory muscle disorder [4]. TMD, reported to affect approximately 31% of adults and elderly individuals and 11% of children and adolescents is characterized by facial and preauricular pain, joint noise, limited jaw movement, and, in severe cases, oral-stage dysphagia [5]. Despite advances in understanding and managing TMD, its diagnosis and treatment remain challenging, highlighting the need for further investigation into its pathological mechanisms.

Condylar erosion, characterized by reduced cortical surface and subchondral bone density, is a hallmark of intra-articular TMD. This condition is associated with impaired

adaptive capacity and disease progression [6]. The LP muscle, a two-headed muscle in the infratemporal fossa, plays a significant role in TMJ function. A small portion of the upper head of the LP inserts into the anteromedial surface of the TMJ capsule and the anterior edge of the TMJ disc. Most of the upper head muscle fibers, and those from the lower head are inserted into the pterygoid fovea on the neck of condyles [7]. Involuntary contractions of the LP can lead to uncontrolled mandibular movements [8].

Pathological changes in the LP muscle, such as hypermyofunction, muscle spasms, impaired coordination between its upper and lower heads, and compromised control and stability of the TMJ, are commonly observed in TMD patients [9]. Restoring LP muscle function is thus essential for the management of TMD. However, the role of the LP in influencing the mandibular condyles, remains insufficiently understood. Recent studies suggest that Botox injections in the LP muscle may help alleviate TMD-associated symptoms [10]. However, limited evidence exists on the impact of Botox on the mandibular condyles through its regulation of LP muscle symmetry.

This study aimed to investigate the effects of Botox A on the LP muscle and its influence on condylar subchondral bone mass.

Materials and Methods

Experimental Animals

Forty-eight 6-week-old male Sprague-Dawley (SD) rats (200 ± 20 g) were obtained from the Sichuan Laboratory Animal Testing Center (License No. SCXK (Sichuan) 20015-030). The rats were randomly assigned to experimental and control groups in a 1:1 ratio. Prior to experimentation, rats were acclimatized in a controlled environment (temperature: 22–25 °C, relative humidity: 50%–60%, light/dark cycle: 12/12 h) for at least one week with ad libitum access to sterile tap water and SPF-grade feed. All animal experiments in this study were approved by the Animal Experimental Ethics Committee of Kunming Medical University (Approval No: KMMU20221618). All procedures were conducted following the guidelines of the China Council on Animal Care and Use.

Main Equipment and Reagents

A micro-computed tomography (Micro-computed tomography (CT)) system (Quantum GX, PerkinElmer Demonstration Laboratory, Shanghai Medical College, Fudan University, Shanghai, China) and the Caliper Micro-CT Analyzer software (Bruker Corp, Allentown, Pennsylvania, USA) were used for imaging and analysis. Microsyringes (7655-01, 50 µL, Hamilton, Bonaduz, Switzerland) were utilized for injecting Botox A (Allergan, Dublin, Ireland). A tartrate-resistant acid phosphatase (TRAP) staining kit (387A, Sigma-Aldrich, St. Louis, MO, USA) was applied for osteoclast staining.

Botox A Treatment

All rats fasted overnight before the procedure. Botox A was diluted in normal saline to a concentration of 2.5 U/0.1 mL [11].

Inhalational anesthesia using 1–3% isoflurane (R510-22-10, RWD, Shenzhen, China) with an anaesthesia gas machine (SF-B01; MR Technology, Inc., Tsukuba, Ibaraki, Japan), the rats were placed in a left decubitus position, and the area from the right outer eyelid to the anterior region of the right ear was shaved. At the midpoint of the upper edge of the zygomatic arch, approximately 7 mm anterior to the tragus, a microsyringe was inserted perpendicularly to the temporal side of the skin, penetrating deeply until the needle reached the bone surface of the squamous portion of the temporal bone, with a depth of 8 mm. The needle was then retracted slightly, angled at 30° to the line connecting the right outer eyelid and the anterior right ear region, and re-inserted backward and inward to a depth of 8 mm.

In the experimental group, 40 µL of Botox A solution was injected slowly when resistance indicative of muscle penetration was felt, and no blood reflux was observed. Following the same procedure, the control group received an equivalent (40 µL) of normal saline. All rats were euthanized via cervical dislocation under deep anesthesia at 2-, 4-, 8-, and 12-weeks post-injection, and the right TMJ samples were excised for subsequent assays.

Micro-CT Analysis

The microarchitecture of the condylar samples was analyzed using a calibrated Micro-CT system. The scan parameters were set at 90 kV and 88 µA, with a 360° rotation and an imaging field of 36 mm. Data were acquired with a voxel size of 72 µm, and each TMJ scan lasted approximately 14 minutes. After three-dimensional (3D) reconstruction of the scanning data, representative second-dimension (2D) and 3D images of the TMJ condylar head (cubic regions of interest: 0.5 mm × 0.5 mm × 0.5 mm) were selected. Bone parameters, including trabecular number (Tb.N), trabecular thickness (Tb.Th), bone volume fraction (BV/TV), trabecular space (Tb.Sp), and the ratio of bone surface area to bone volume (BS/BV), were analyzed using Caliper Analyzer software (Caliper; Hopkinton, MA, USA).

Tartrate-Resistant Acid Phosphatase (TRAP) Staining

Mandibular condyles were fixed in 10% formalin (HT501128, Sigma-Aldrich, St. Louis, MO, USA) at room temperature for 24 hours, washed with 0.01 M phosphate buffer saline (PBS) (pH 7.3), and decalcified in 10% ethylene diamine tetraacetic acid (EDTA) decalcification solution at 4 °C. The decalcification solution was refreshed daily, and the tissue was punctured with a syringe needle to facilitate the process. Decalcification was terminated when no resistance was detected.

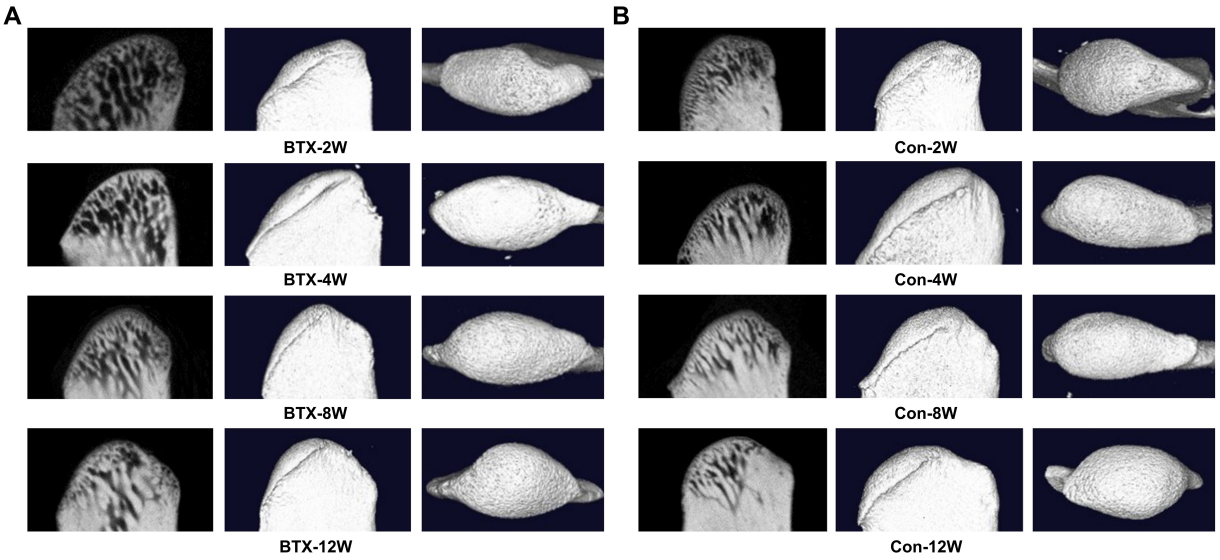

Fig. 1. Representative Micro-CT analysis of condylar subchondral bones in rats treated with experimental group (BTX) and control (Con) groups at 2-, 4-, 8-, and 12-weeks. (A) Experimental group (BTX). (B) Control (Con) group. Two-dimensional, three-dimensional, and top-view three-dimensional images of the condylar subchondral bone are shown. n = 6 in each group.

The samples were dehydrated, embedded in paraffin, and sectioned into 4-µm slices. Sections were preheated in deionized water at 37 °C. The staining solution was prepared by mixing 0.5 mL fast garnet GBC base solution and 0.5 mL sodium nitrate solution in a centrifuge tube for 30 seconds, then allowing it to stand for 2 minutes. The mixture was combined with additional reagents (45 mL preheated deionized water at 37 °C, 1 mL mixed solution, 1 mL GBC solution, 0.5 mL Naphthol AS-BI phosphate, 2 mL acetate solution, and 1 mL tartrate solution).

The sections were immersed in the prepared solution, incubated at 37 °C for 1 hour in the dark, washed with deionized water, and counterstained with hematoxylin (C0107, Beyotime, Shanghai, China) for 2 minutes. After washing with PBS, the sections were sealed. For each group and time point, three sections were randomly selected. Images were captured using a light microscope (×400, AXio Lab.A1, ZEISS, Oberkochen, Germany), and the number of osteoclasts was manually counted and statistically analyzed.

Hematoxylin-Eosin (HE) Staining

Murine mandibular condyles sections (4 µm) were dewaxed and rehydrated, followed by sequential staining with hematoxylin for 5 minutes and eosin for 1 minute (C0109, Beyotime, Shanghai, China) at room temperature. The morphology of the TMJ samples was then observed under a light microscope (Zeiss, Jena, Germany) at ×400 magnification.

Western Blotting

Protein supernatants were extracted by lysing tissues in radioimmunoprecipitation assay (RIPA) buffer (C500007, Sangon, Shanghai, China) and centrifuging at 12,830 ×g for 5 minutes at 4 °C. Protein concentrations were measured using bicinchoninic acid (BCA) assay (C503021, Sangon, Shanghai, China). Equal amounts of protein (45 µg per sample) and 5 µL of marker (PR1910, Solarbio, Beijing, China) were separated through SDS-PAGE (C631100, Sangon, Shanghai, China) and transferred to polyvinylidene fluoride (PVDF) membranes (F019533, Sangon, Shanghai, China). The membranes were blocked with 5% bovine serum albumin (BSA; E661003, Sangon, Shanghai, China) for 1 hour at room temperature and incubated overnight at 4 °C with the following primary antibodies: TRAP (1:500; ab65854, 32 kDa, Abcam, Cambridge, UK), osteocalcin (OCN) (1:1000; PA5-96529, 13 kDa, Thermo Fisher Scientific, Waltham, MA, USA), type I collagen (COL1A1) (1:1000; ab270993, 139 kDa, Abcam, Cambridge, UK), and glyceraldehyde-3-phosphate dehydrogenase (GAPDH) (1:10,000; ab181602, 36 kDa, Abcam, Cambridge, UK). After washing, the membranes were incubated with secondary antibodies (anti-rabbit IgG, ab205718, 1:2000, Abcam, Cambridge, UK) for 1 hour at room temperature.

Protein bands were visualized using enhanced chemiluminescence (ECL) reagents (C510043, Sangon, Shanghai, China) and captured with a GelView 6000Plus Smart Gel Imaging System (Biolight Biotechnology, Guangzhou, China). Qualitative analysis was performed using the Image Quant LAS 4000 system (GE Healthcare, Marlborough, MA, USA) equipped with ImageJ software (v2.0.0, NIH, Bethesda, MD, USA).

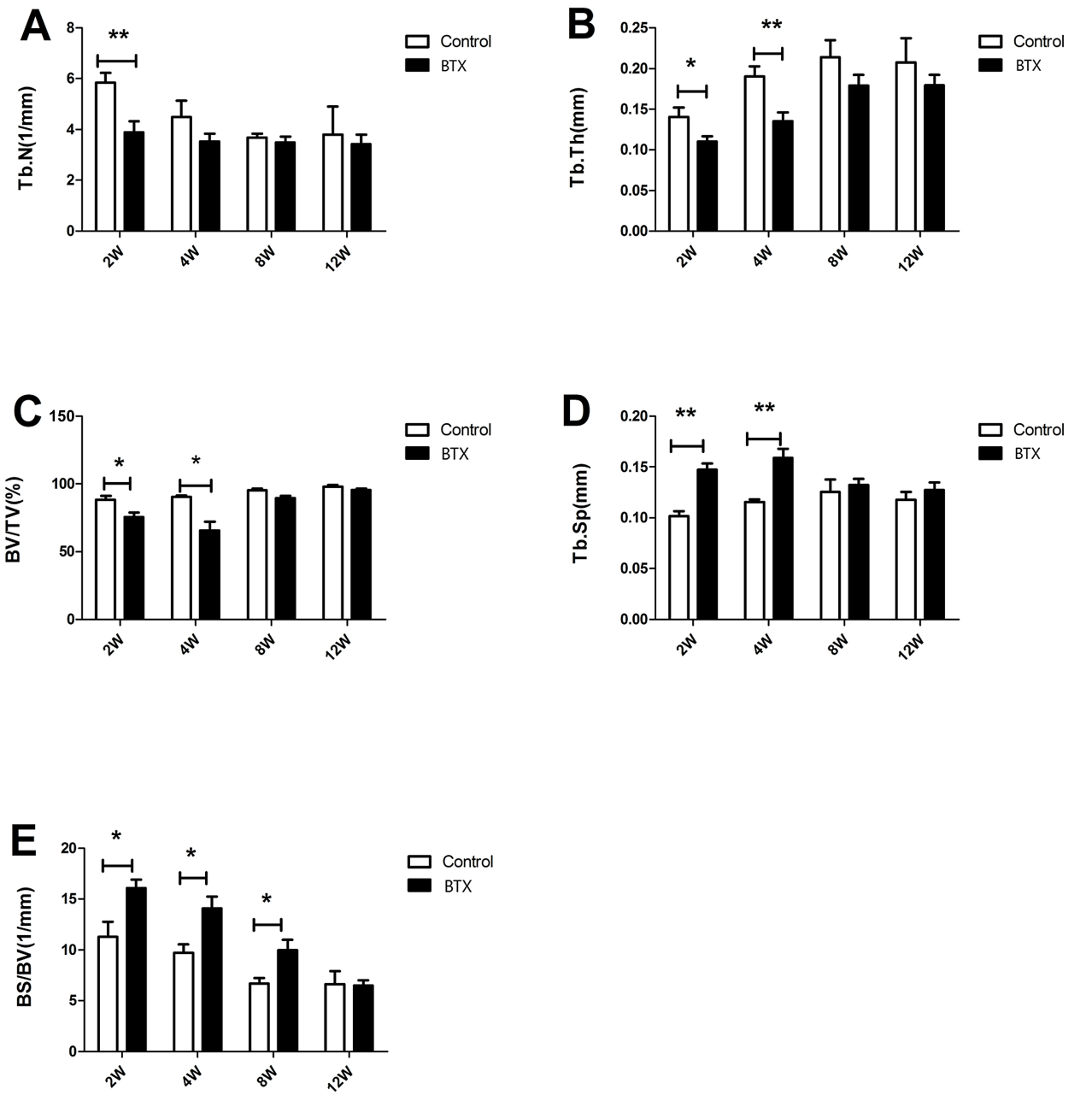

Fig. 2. Quantitative analysis of three-dimensional microstructural parameters of condylar subchondral bone. (A) Trabecular number (Tb.N). (B) Trabecular thickness (Tb.Th). (C) Bone volume fraction (BV/TV). (D) Trabecular space (Tb.Sp). (E) Bone surface area-to-bone volume ratio (BS/BV). *$p < 0.05$, **$p < 0.01$, vs. control. n = 6 in each group.

Statistical Analysis

Statistical analyses were conducted using SPSS software (version 24.0, IBM Corporation, Armonk, NY, USA). All measurement data were expressed as mean ± standard deviation (SD). Normality was assessed using the Shapiro-Wilk test. Comparisons between the two groups were conducted using independent samples *t*-tests. A *p*-value < 0.05 was considered statistically significant.

Sample size calculation was based on the primary outcome, "condyle width", as reported in a similar previous study due to a lack of direct data matching the specific outcomes of this study [12]. Using PASS software (PASS 15, NCSS, LLC, Kaysville, UT, USA), it was assumed that the condyle width was 2.95 ± 0.13 mm in the experimental group and 3.19 ± 0.14 mm in the control group. Parameters for the calculation were set as follows: equal sample sizes (1:1 ratio), power = 0.9, $\alpha = 0.05$, and a dropout rate of 25%. The calculation indicated a requirement of 11 samples per group (22 samples in total). To account for potential variability, 24 rats in each group were enrolled, resulting in a total of 48 rats.

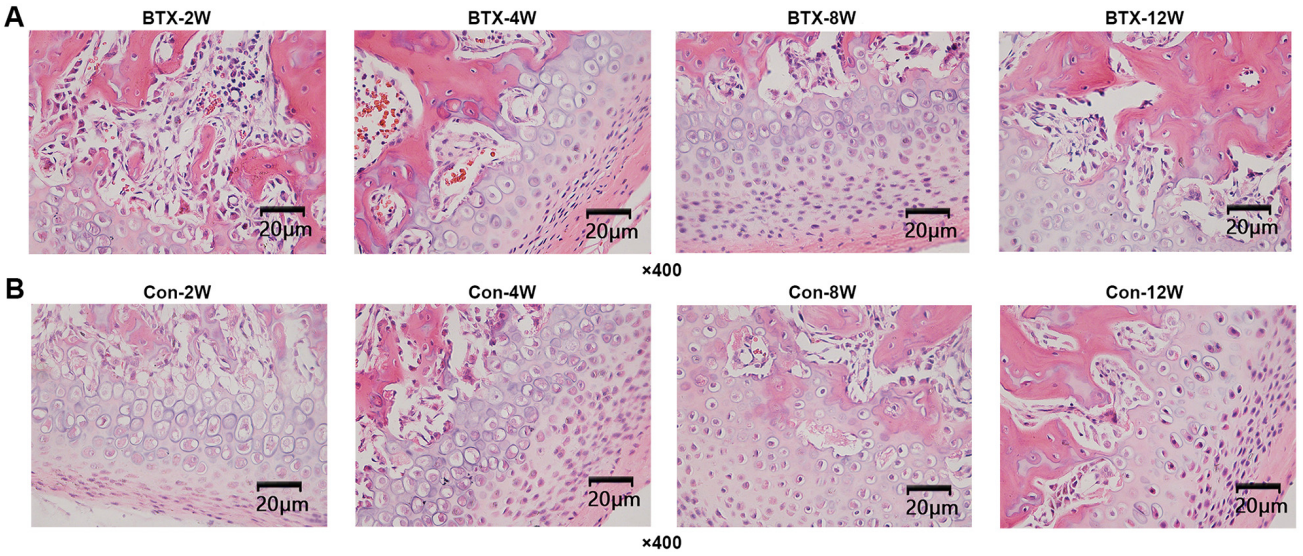

Fig. 3. Hematoxylin-eosin (HE) staining of condylar subchondral bone in rats at weeks 2, 4, 8, and 12. (A) Representative images illustrate histological changes in subchondral bone following Botox A (BTX) treatment. (B) Representative images illustrate histological changes in subchondral bone in the control (Con) group. Magnification: ×400. n = 6 in each group.

Results

Early Botox Injection Induces Bone Loss in the Rat Mandibular Condyles

Botox A was injected into the right lateral pterygoid muscle of rats, and changes in bone mass of the right condyles were evaluated using Micro-CT at 2-, 4-, 8-, and 12-weeks post-injection (Fig. 1). At 2-weeks post-injection, Tb.N, Tb.Th, and BV/TV values in the experimental group were significantly lower compared to the control group ($p < 0.05$; Fig. 2A–C), while Tb.Sp and BS/BV were significantly higher ($p < 0.05$; Fig. 2D,E). At 4-weeks post-injection, Tb.Th and BV/TV values remained significantly lower ($p < 0.05$; Fig. 2B,C), and Tb.Sp and BS/BV values were significantly higher ($p < 0.05$; Fig. 2D,E) in the experimental group compared to the control group. However, no significant differences in Tb.N were observed between groups at this time point ($p > 0.05$; Fig. 2A).

At 8-weeks post-injection, no significant differences in Tb.N, Tb.Th, BV/TV or Tb.Sp were observed between the experimental and control groups ($p > 0.05$; Fig. 2A–D). However, the BS/BV ratio remained significantly higher in the experimental group ($p < 0.05$; Fig. 2E). By 12-weeks post-injection, no significant differences in Tb.N, Tb.Th, BV/TV, Tb.Sp or BS/BV were detected between the experimental and control groups ($p > 0.05$; Fig. 2A–E).

Early Botox A Injection Causes Condylar Subchondral Bone Damage in Rats

Hematoxylin-eosin (HE) staining was performed to analyze the pathological changes in the condylar subchondral bone following Botox A injection. At 2-weeks post-injection, the experimental group exhibited fractures and exfoliation of the fibrous layer, increased cell proliferation in the proliferative layer, thinning of the hypertrophic layer, and uneven cell distribution compared to the control group (Fig. 3A). Sparse and fractured trabecular bone in the experiment group was observed in the subchondral region, with erythrocytes and inflammatory cells in the matrix (Fig. 3A). In contrast, condylar samples in the control group showed smooth and intact cartilage surfaces, evenly distributed cells, and clear stratification (Fig. 3B).

By 4-weeks post-injection, condylar samples in the experimental group displayed a significant reduction in the number of cells within the hypertrophic cartilage layer, fractures in the subchondral bone trabeculae, and aggregation of erythrocytes and inflammatory cells in the stroma compared to the control group (Fig. 3A). At 8-weeks post-injection, the experimental group displayed fewer cells in the hypertrophic cartilage layer, sparse trabecular gaps, and mild fractures of the subchondral trabecular bone compared to the control group (Fig. 3A). By 12-weeks post-injection, the subchondral bone morphology in the experimental group was largely restored and comparable to that of the control group (Fig. 3A).

Early Botox A Injection Enhances Osteoclast Activity and Alters Subchondral Bone Remodeling in Rat Mandibular Condyles

To investigate the impact of Botox A on osteoclast activity, TRAP staining was performed to evaluate osteoclast formation in the condylar subchondral bones at 2-, 4-, 8-, and 12-weeks post-injection. At 2-weeks post-injection, condylar samples from the experimental group showed a significant increase in the presence of large, multinucleated osteoclasts with irregular morphology and heightened ac-

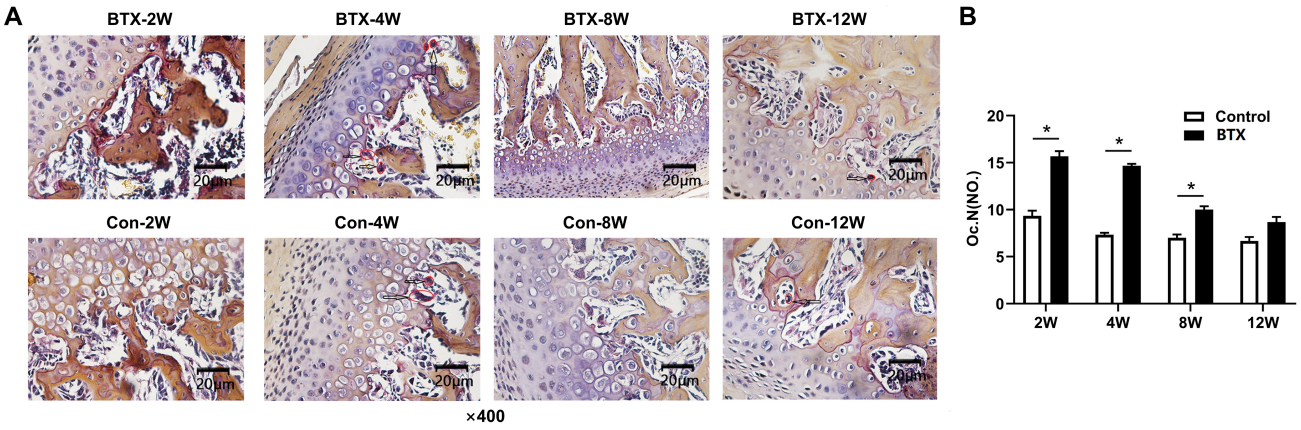

Fig. 4. Visualization of osteoclasts in rat condylar subchondral bone via tartrate-resistant acid phosphatase (TRAP) staining. (A) Representative TRAP-stained images of condylar subchondral bone at weeks 2, 4, 8, and 12 post-treatments. Arrows indicate osteoclasts. (B) Quantification of osteoclast numbers in TRAP-stained sections of the condylar subchondral bone of condyle at the indicated time points. Magnification: ×400. Data are presented as mean ± SD. *$p < 0.05$, vs. Control. BTX, Botox A; n = 6 in each group.

tivity at the cartilage-subchondral bone interface compared to the control group ($p < 0.05$; Fig. 4).

By 4-weeks post-injection, the experimental group sustained an elevated number of osteoclasts at the cartilage and subchondral bone junction, accompanied by well-organized columnar osteoblasts ($p < 0.05$; Fig. 4). At 8-weeks post-injection, an increased number of osteoclasts remained evident in the experimental group at the cartilage-subchondral bone interface compared to the control group ($p < 0.05$; Fig. 4). However, 12-weeks post-injection, the number of osteoclasts in the experimental group showed no significant difference compared to the control group ($p > 0.05$; Fig. 4).

Osteoclast and Osteoblast Activities in Rat Mandibular Condyles

To further examine the bone remodeling process, the expression levels of OCN and COL1A1, key markers of osteoblast activity, were assessed by western blotting. In the experimental group, OCN and COL1A1 expression, primarily localized to the trabecular bone surface, significantly increased at 8 and 12 post-injections compared to the control group ($p < 0.05$; Fig. 5A–C). TRAP protein levels, indicative of osteoclast activity, were significantly elevated in the experimental group at 2-, 4-, and 8-weeks post-injection ($p < 0.01$; Fig. 5A,D). By 12-weeks post-injection, TRAP protein levels returned to baseline, comparable to the control group.

Discussion

LP muscle is essential in mandibular function, facilitating forward and downward movement of the condyle and articular disc while stabilizing and coordinating the disc-condyle complex during mandibular opening and closing. Unlike the masseter and temporalis muscles, which are more accessible due to their superficial location and larger attachment areas, the LP muscle is situated in a deeper anatomical position, making it challenging to access directly [13]. Barriers to *in vitro* injection include anatomical constraints, and intraoral approaches are further complicated by the presence of the tongue, making accurate injections difficult.

Previous studies have explored the role of the LP muscle in mandibular biomechanics. For example, a sheep model was selected to investigate the effect of LP muscle on the healing of condylar sagittal fracture by surgically severing the muscle to impair its function [14]. Similarly, a rat model of masticatory muscle imbalance was created by unilateral masseter muscle resection, which revealed suppressed condylar cartilage formation and asymmetrical condylar process development [15]. Muscle dysfunction has also been associated with systemic conditions and hormonal influences, making it susceptible to relapse and aggravation due to multiple factors [16]. To minimize such confounding factors, male animals were used in this study to eliminate the potential effects of estrogen.

To simulate the condition of LP muscle injury in patients with unilateral masseter muscle dysfunction and evaluate its effects on condylar subchondral bone mass, an animal model of LP muscle imbalance was established in SD rats via extraoral injection of Botox A into the LP muscle. This experimental approach offers several advantages, including minimal invasiveness and the use of reversible drugs.

Botox A paralyzes autonomic muscle tissue through inhibition of acetylcholine release at the neuromuscular junction [17]. Injection of Botox A into the LP muscle is considered a safe and effective method to treat chronic TMJ dislocation [9,18]. This minimally invasive treatment improves the quality of life for patients with cephalic and facial disorders of various etiologies and has relatively fewer

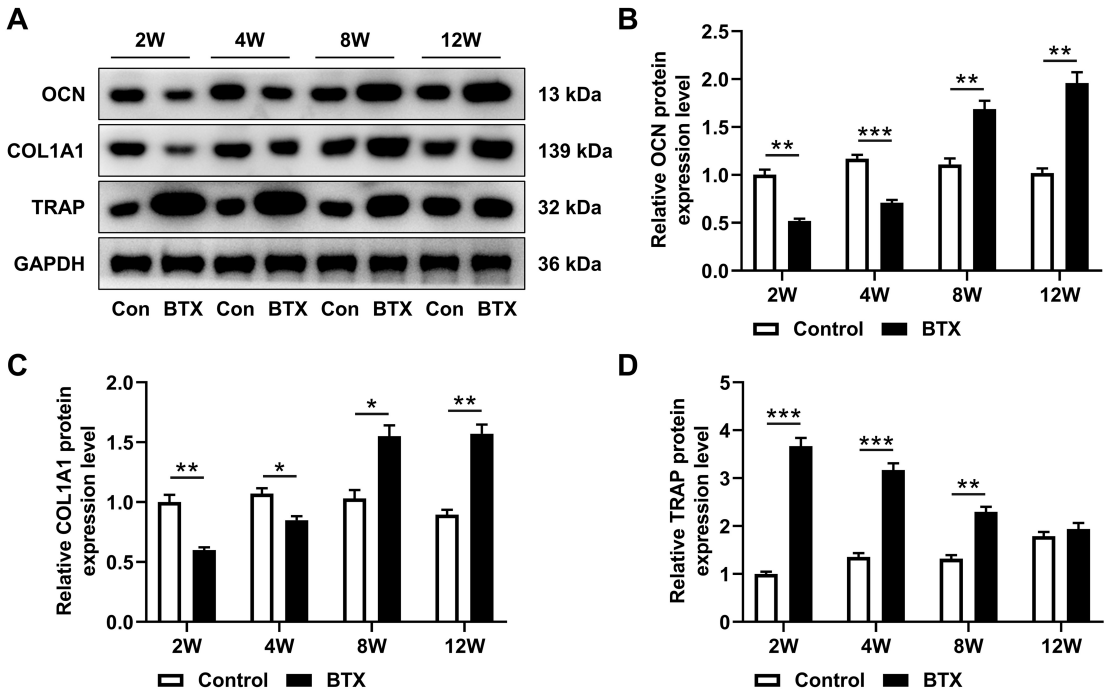

Fig. 5. Protein expression levels of osteoclast and osteoblast markers in rat mandibular condyles assessed by western blotting. (A) Representative western blotting images showing bands for TRAP, osteocalcin (OCN), and type I collagen (COL1A1), with glyceraldehyde-3-phosphate dehydrogenase (GAPDH) as a loading control. (B–D) Quantitative analysis of OCN, COL1A1, and TRAP protein levels in mandibular condyles at various time points. Data expressed as mean ± SD. BTX, Botox A; Con, Control. *$p < 0.05$, **$p < 0.01$, ***$p < 0.001$ vs. Control. n = 3 in each group.

side effects [19]. However, a study reported that Botox A injection into the masseter muscle of rats results in significant impairment of cortical and trabecular bone in the condyle [20]. While Botox injection effectively manages various dyskinesia [21], its precise mechanisms of action remain incompletely understood.

One study showed that Botox reduces pain and sensitivity in patients with persistent myofascial pain. However, adverse reactions such as reduced masticatory performance, decreased muscle thickness, and mandibular bone volume loss have been documented [22]. Compared to traditional therapies, Botox A offers a more targeted approach to managing TMJ-related disorders by directly intervening in pathological processes. Due to its reversible and time-limited effects, Botox A injection is usually repeated at 3–6-month intervals. The mechanism of Botox A involves the temporary failure of affected nerves to stimulate muscle contraction. Over time, as the drug is metabolized and nerve endings regenerate, the affected nerves re-innervate their target muscles, gradually restoring their function, thus rendering Botox A ineffective. The onset of action for Botox A typically occurs within 3–7 days (most commonly 1–3 days), peaks 1–2 weeks post-injection, and then transitions to a weaker but stable effect lasting 3–6 months [23]. However, individual differences in drug efficacy remain a notable factor.

In the present study, experimental time points were set at 2-, 4-, 8-, and 12-weeks, within the range of Botox A efficacy. Occlusal changes in the SD rats were evident at 2-weeks post-injection, consistent with the peak effect of the drug. At 4-weeks, clinical signs in the experimental group worsened, likely due to further occlusal disturbances associated with the induced muscle strength imbalance. Recovery began at 8-weeks, and by 12-weeks, normalization of occlusal parameters was observed, suggesting a gradual restoration of muscle and bone dynamics as the effects of Botox A subsided.

A systematic review by Michael Owen *et al.* [24] highlighted significant alterations in mandibular bone mass following Botox A injection into the masticatory muscle. The condylar head and rostral process were identified as the most frequently affected regions, with prominent changes in cortical bone thickness and trabecular bone density. Despite the extensive data on bone quality alterations following Botox A injection, critical knowledge gaps remain about the variables influencing them [24]. Therefore, the article also emphasized the need for further investigation into dose-dependent effects and the impacts of factors such as gender and age on mandibular bone quality.

Subchondral bone exhibits considerable adaptability, with its morphology, thickness, density, vascularization, biochemical composition, and mechanical properties undergoing reconstruction in response to environmental

changes [25]. The thickness of the subchondral bone is directly influenced by the stress applied to the articular surface, indicating that its morphology is functionally determined by cartilage surface activity [26]. The trabecular bone, located beneath the subchondral bone plate, provides structural support [25]. Micro-CT has emerged as a reliable method to quantify bone loss and visualize 3D structures. The technique is widely used to assess bone quality and morphology in small animal models under physiological and pathological conditions and the fine structure of bone and cartilage [27].

In this study, Micro-CT analysis revealed a significant reduction in BV/TV at 2- and 4-weeks in the experimental group. These findings indicate that subchondral bone formation was suppressed during the early stages post-injection. Conversely, BS/BV was significantly higher in the experimental group at 2-, 4-, and 8-weeks than in the control group, suggesting an enhanced subchondral bone remodeling capacity during these time points.

A previous study [28] investigating the cellular and matrix responses of condylar cartilage and subchondral bone to Botox A demonstrated significant reductions in BV/TV, tissue density of subchondral bone, and Tb.Th on the side of the condyle receiving the Botox injection. Additionally, the experimental group exhibited elevated apoptosis rates among subchondral osteocytes and chondrocytes, which is consistent with the findings from our study.

Further research on age-related changes in cancellous bone microstructure revealed that aging prominently increases the bone marrow volume and BS/BV while reducing the BV/TV, average bone trabecula volume, and bone surface density. These findings reflect the remodeling mechanisms underlying bone aging [29]. In our study, no significant differences in these parameters were observed at 8- and 12-weeks, likely due to the combined effect of Botox A metabolism and age-related factors. These observations suggest that the aging of mice may be associated with increased BS/BV and decreased BV/TV values.

Mastication is influenced by the masticatory cycle, duration, onset, and amplitude of muscle activity. Following 2- and 4-weeks of modeling, a significant reduction in the hypertrophic cartilage layer cells of the condylar cartilage was observed. In certain areas, the subchondral bone of the condylar cartilage was directly connected to the proliferative cartilage layer. This was attributed to a marked decrease in type II collagen and proteoglycan content in the cartilage layer, resulting in a thinner hypertrophic cartilage layer. Additionally, the previously rugged “tidal line” the subchondral bone and cartilage junction became noticeably smoother. Subchondral bone is richly innervated and vascularized, supplying critical nutrients to the cartilage. An imbalance between osteogenesis and osteoclast activity can lead to subchondral bone remodeling. In this study, at 8- and 12-weeks post-modeling, improvement in condylar bone mass loss was evident. These findings reflect the restoration of a dynamic balance between osteogenesis and osteoclasts in the body. However, the precise mechanism underlying these observations, including the potential involvement of cellular signaling pathways and gene regulation, requires further investigation.

Conclusions

In conclusion, our findings demonstrated a time-dependent recovery in condylar subchondral bone mass in rats following initial loss in the early phase after Botox A injection into a single LP muscle. These findings provide insights into the dynamic changes in subchondral bone remodeling associated with localized muscle function.

Availability of Data and Materials

The datasets used and/or analyzed during the current study are available from the corresponding authors upon reasonable request.

Author Contributions

LT and YH designed the research study; WZ, WY and CJ, performed the research; DH, EM, YL and XS collected and analyzed the data. LT and YH have been involved in drafting the manuscript and all authors contributed significantly to editorial changes of important content. All authors gave final approval of the version to be published. All authors have participated sufficiently in the work to take public responsibility for appropriate portions of the content and agreed to be accountable for all aspects of the work in ensuring that questions related to its accuracy or integrity.

Ethics Approval and Consent to Participate

All animal experiments in this study were approved by the Animal Experimental Ethics Committee of Kunming Medical University (Approval No: KMMU20221618). All procedures were conducted following the guidelines of the China Council on Animal Care and Use.

Acknowledgment

Not applicable.

Funding

This research received no external funding.

Conflict of Interest

The authors declare no conflict of interest.

References

[1] Muraoka H, Kaneda T, Ito K, Hirahara N, Kondo T, Tokunaga S. Quantitative analysis of masticatory muscle changes by Eichner index using diffusion-weighted imaging. Oral Radiology. 2023; 39: 437–445.

[2] Hatcher DC. Anatomy of the Mandible, Temporomandibular Joint, and Dentition. Neuroimaging Clinics of North America. 2022; 32: 749–761.

[3] Kalladka M, Young A, Thomas D, Heir GM, Quek SYP, Khan J. The relation of temporomandibular disorders and dental occlusion: a narrative review. Quintessence International. 2022; 53: 450–459.

[4] Romero-Reyes M, Bassiur JP. Temporomandibular Disorders, Bruxism and Headaches. Neurologic Clinics. 2024; 42: 573–584.

[5] Gilheaney Ó, Béchet S, Kerr P, Kenny C, Smith S, Kouider R, *et al*. The prevalence of oral stage dysphagia in adults presenting with temporomandibular disorders: a systematic review and meta-analysis. Acta Odontologica Scandinavica. 2018; 76: 448–458.

[6] Ulay G, Pekiner FN, Orhan K. Evaluation of the relationship between the degenerative changes and bone quality of mandibular condyle and articular eminence in temporomandibular disorders by cone beam computed tomography. Cranio. 2023; 41: 218–229.

[7] Ueki K, Moroi A, Takayama A, Yoshizawa K. Change of lateral pterygoid muscle and temporomandibular disc position after bimaxillary surgery in class II and III patients. Oral and Maxillofacial Surgery. 2021; 25: 19–25.

[8] Lee S-T, Kim D, Park J-H, Kwon T-G. Ultrasound-guided intraoral botulinum toxin injection into the lateral pterygoid muscle for chronic temporomandibular joint dislocation. Journal of the Korean Association of Oral and Maxillofacial Surgeons. 2024; 50: 41-48.

[9] Rezazadeh F, Esnaashari N, Azad A, Emad S. The effects of botulinum toxin A injection on the lateral pterygoid muscle in patients with a painful temporomandibular joint click: a randomized clinical trial study. BMC Oral Health. 2022; 22: 217.

[10] Blanco-Rueda JA, López-Valverde A, Márquez-Vera A, Méndez-Sánchez R, López-García E, López-Valverde N. Preliminary Findings of the Efficacy of Botulinum Toxin in Temporomandibular Disorders: Uncontrolled Pilot Study. Life. 2023; 13: 345.

[11] Wen WD, Yuan F, Hou YP. The mechanism of inhibitory effect on parotid gland secretion with local injection of botulinum toxin type A in the rat. Chinese Journal of Stomatology. 2009; 44: 38–40. (In Chinese)

[12] Dutra EH, O' Brien MH, Lima A, Kalajzic Z, Tadinada A, Nanda R, *et al*. Cellular and Matrix Response of the Mandibular Condylar Cartilage to Botulinum Toxin. PLoS ONE. 2016; 11: e0164599.

[13] Zebovitz E. Total Temporomandibular Joint Prosthetic Reconstruction: The Importance of Lateral Pterygoid Muscle Reattachment to Lateral Excursive and Protrusive Mandibular Movement. Journal of Oral and Maxillofacial Surgery. 2021; 79: 1191–1194.e1.

[14] Wu D, Yang XJ, Cheng P, Deng TG, Jiang X, Liu P, *et al*. The lateral pterygoid muscle affects reconstruction of the condyle in the sagittal fracture healing process: a histological study. International Journal of Oral and Maxillofacial Surgery. 2015; 44: 1010–1015.

[15] Miyazaki M, Yonemitsu I, Takei M, Kure-Hattori I, Ono T. The imbalance of masticatory muscle activity affects the asymmetric growth of condylar cartilage and subchondral bone in rats. Archives of Oral Biology. 2016; 63: 22–31.

[16] Greco F, Moulton C, Antinozzi C, Lista M, Di Luigi L, Dimauro I, *et al*. Relationship between Euthyroidism and Muscle Mass and Strength: A Systematic Review. International Journal of Sports Medicine. 2023; 44: 704–710.

[17] Gatti V, Ghobryal B, Gelbs MJ, Gerber MB, Doty SB, Cardoso L, *et al*. Botox-induced muscle paralysis alters intracortical porosity and osteocyte lacunar density in skeletally mature rats. Journal of Orthopaedic Research. 2019; 37: 1153–1163.

[18] Emara AS, Faramawey MI, Hassaan MA, Hakam MM. Botulinum toxin injection for management of temporomandibular joint clicking. International Journal of Oral and Maxillofacial Surgery. 2013; 42: 759–764.

[19] Brin MF, Burstein R. Botox (onabotulinumtoxinA) mechanism of action. Medicine. 2023; 102: e32372.

[20] Matthys T, Ho Dang HA, Rafferty KL, Herring SW. Bone and cartilage changes in rabbit mandibular condyles after 1 injection of botulinum toxin. American Journal of Orthodontics and Dentofacial Orthopedics. 2015; 148: 999–1009.

[21] Jankovic J. An update on new and unique uses of botulinum toxin in movement disorders. Toxicon. 2018; 147: 84–88.

[22] De la Torre Canales G, Alvarez-Pinzon N, Muñoz-Lora VRM, Vieira Peroni L, Farias Gomes A, Sánchez-Ayala A, *et al*. Efficacy and Safety of Botulinum Toxin Type A on Persistent Myofascial Pain: A Randomized Clinical Trial. Toxins. 2020; 12: 395.

[23] Wang L, Ringelberg CS, Singh BR. Dramatic neurological and biological effects by botulinum neurotoxin type A on SH-SY5Y neuroblastoma cells, beyond the blockade of neurotransmitter release. BMC Pharmacology & Toxicology. 2020; 21: 66.

[24] Owen M, Gray B, Hack N, Perez L, Allard RJ, Hawkins JM. Impact of botulinum toxin injection into the masticatory muscles on mandibular bone: A systematic review. Journal of Oral Rehabilitation. 2022; 49: 644–653.

[25] Cardoneanu A, Macovei LA, Burlui AM, Mihai IR, Bratoiu I, Rezus II, *et al*. Temporomandibular Joint Osteoarthritis: Pathogenic Mechanisms Involving the Cartilage and Subchondral Bone, and Potential Therapeutic Strategies for Joint Regeneration. International Journal of Molecular Sciences. 2022; 24: 171.

[26] Hu W, Chen Y, Dou C, Dong S. Microenvironment in subchondral bone: predominant regulator for the treatment of osteoarthritis. Annals of the Rheumatic Diseases. 2021; 80: 413–422.

[27] Shim J, Iwaya C, Ambrose CG, Suzuki A, Iwata J. Microcomputed tomography assessment of bone structure in aging mice. Scientific Reports. 2022; 12: 8117.

[28] Hou S, Peng S, Dai H, Song J, Xu L, Zhou J, *et al*. Mechanical loading and autophagy: A study on the BoNT-A injection-induced condylar cartilage degeneration. Archives of Biochemistry and Biophysics. 2023; 749: 109788.

[29] Ries C, Boese CK, Stürznickel J, Koehne T, Hubert J, Pastor MF, *et al*. Age-related changes of micro-morphological subchondral bone properties in the healthy femoral head. Osteoarthritis and Cartilage. 2020; 28: 1437–1447.